Atomic Scale Friction: What can be Deduced from the Response to a Harmonic Drive?

V. Zaloj,* M. Urbakh, and J. Klafter
School of Chemistry, Tel Aviv University, 69978, Tel Aviv, Israel
(Received 7 April 1998)

In this Letter we investigate the response of a confined chain to a harmonic driving force. A model is introduced which mimics recent measurements on friction using surface forces apparatus. The model predicts a critical driving amplitude below which the response is linear. For higher amplitudes the system exhibits a nonlinear behavior and shear thinning. A novel origin for the thinning is proposed which stems from energy dissipation due to stick-slip motion and the transition to smooth sliding. We establish relationships between the microscopic parameters of the system and phenomena observed in rheology and tribology. [S0031-9007(98)06799-4]

PACS numbers: 46.30.Pa, 68.45.–v, 81.40.Pq

There has been a growing number of attempts to understand the relationship between frictional forces and the microscopic properties of nanosystems. Recent studies on friction [1–9] have exposed a broad range of phenomena and new behaviors which help shed light on some "old" concepts which are already considered textbook material. These include the static and kinetic friction forces, transition to sliding, and thinning, which have been widely discussed but whose microscopic meaning is still lacking.

There have been, generally, two approaches used to investigate shear forces of confined liquids: rheological (oscillatory external drive) and tribological (constant driving velocity). In the bulk the two approaches lead to similar results, but less is known about the relationship between rheology and tribology in nanoscale confined systems. Establishing a relationship between these approaches is essential for creating a unifying description of the response to shear and for further progress of related fields.

In this Letter we concentrate on the rheological side of the problem and its relationship to tribology. Our proposed predictions can be tested experimentally by simultaneously analyzing the time series of the spring forces and the shear moduli. We suggest an interpretation to the observed dramatic enhancement in the effective viscosity [3,6] and to the effect of shear thinning in thin confined systems [3,10–12].

In order to mimic the commonly used experimental configuration [13] we introduce a model of a chain embedded between two plates, one of which is externally driven, as depicted in Fig. 1a. The top plate of mass M is connected to a spring, of spring constant K_1, which is harmonically driven, and to a spring K_2, which is a response spring. The chain consists of N identical particles each of mass m_0, which interact harmonically. The dynamical behavior of the system (chain + plates) follows the equations of motion:

$$M\ddot{X} + \eta_0 \sum_{i=1}^{N} (X - \dot{x}_i) + K_1[X - X_d(t)] + K_2 X + \sum_{i=1}^{N} \frac{\partial U(x_i - X)}{\partial X} = 0, \tag{1a}$$

$$m_0 \ddot{x}_i + \eta_0 (2\dot{x}_i - \dot{X}) + \sum_{i \neq j} \frac{\partial V(x_i - x_j)}{\partial x_i} + \frac{\partial [U(x_i) + U(x_i - X)]}{\partial x_i} = 0, \qquad i = \overline{1, N}. \tag{1b}$$

Here the coordinate of the harmonically driven stage is $X_d(t) = X_{dm} \sin(\omega_d t)$. The microscopic parameter η_0 is responsible for the dissipation of the kinetic energy of each particle. $U(x) = -U_0 \cos(2\pi x/b)$ represents the particle-plate interaction. We assume that the interparticle interaction is harmonic $V(x_i - x_{i\pm1}) = k(x_i - x_{i\pm1} \mp a)^2/2$; a and b are the periodicities of the undisturbed chain and of the potential $U(x)$, respectively.

Let us introduce the following dimensionless variables and parameters: the coordinates of the top plate $Y = X/b$ and the chain particles $y_i = x_i/b$; the time $\tau = \omega_0 t$, where the $\omega_0 = (2\pi/b)\sqrt{NU_0/M}$ is the frequency of the top plate oscillations in the minima of the potential $U(x)$ for the case of noninteracting particles; $\gamma = N\eta_0/M\omega_0$, which is the dimensionless friction constant, $\varepsilon = Nm_0/M$, the ratio of the chain and top plate masses, $\alpha = \Omega/\omega_0$, the ratio of frequencies of the mechanical free oscillations of the top plate, $\Omega = \sqrt{(K_1 + K_2)/M}$, and ω_0, $\kappa = K_1/(K_1 + K_2)$ the mechanical factor, $\Delta = 1 - (a/b)$ the misfit of the substrate and chain periods, and $\rho = (\omega_c/\omega)^2$, the ratio of the frequencies related to interparticle $\omega_c = \sqrt{k/m_0}$ and particle-plate $\omega = (2\pi/b) \times \sqrt{U_0/m_0}$ interactions.

In rheological experiments the behavior of the system is governed by two dimensionless parameters: The amplitude $A_d = X_{dm}/b$ and frequency $\delta = \omega_d/\omega_0$ of the driving stage. Another relevant quantity is the driving velocity $V_d = A_d\delta$, which is used in rheology to analyze data, and which is relevant when making comparison to tribological results.

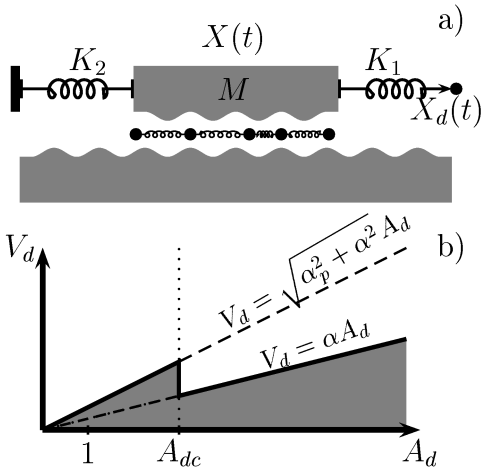

FIG. 1. (a) Schematic representation of the model. The top plate of mass M is driven by a spring K_1 and its displacement is measured by the deflection of the spring K_2. (b) Phase diagram in the dimensionless coordinates (V_d, A_d) for weak spring ($\alpha < 1$).

The drive (K_1) and response (K_2) springs act on the top plate with the dimensionless spring force $f_s(\tau)$ (see Fig. 1a),

$$f_s(\tau) \equiv \frac{F(\tau)}{2\pi F_{0s}} = \alpha^2[\kappa A_d \sin(\delta\tau) - Y(\tau)], \quad (2)$$

where $F_{0s} = 2\pi N U_0/b$ is the static friction force for N noninteracting particles. Under the action of the combined force $f_s(\tau)$, due to the two external springs, the top plate moves by $Y(\tau)$ and acts on the molecular chain with the force $f_c(\tau)$

$$f_c(\tau) = \gamma\left(\dot{Y} - \frac{1}{N}\sum_{i=1}^{N}\dot{y}_i\right) - \frac{1}{2\pi N}\sum_{i=1}^{N}\sin[2\pi(y_i - Y)]$$
$$\equiv f_s(\tau) - \ddot{Y}(\tau). \quad (3)$$

The force $f_c(\tau)$ depends on the driving amplitude A_d, and on the external frequency δ, and is out of phase with respect to the drive. We now introduce complex force amplitudes $\overline{f}_{s(c)} \equiv \overline{f}^{e}_{s(c)} + i\overline{f}^{v}_{s(c)}$ where $\overline{f}^{e}_{s(c)}$ and $\overline{f}^{v}_{s(c)}$ are the sine and cosine Fourier transforms of the $f_{s(c)}(\tau)$. Force amplitudes can be expressed in terms of complex amplitude of the top plate displacement $\overline{Y} = \overline{Y}^{e} + i\overline{Y}^{v}$

$$\overline{f}_c = \overline{f}_s + \delta^2\overline{Y} = \alpha^2[\kappa A_d - \overline{Y}] + \delta^2\overline{Y}. \quad (4)$$

Using the rheological definitions of the complex dynamic modulus of the confined system $G_c = G_c' + iG_c''$ [14] and Eq. (4) we have

$$G_c \equiv \frac{\overline{f_c}}{\overline{Y}} = \alpha^2\left[\kappa\frac{A_d}{\overline{Y}} - 1\right] + \delta^2. \quad (5)$$

The storage modulus G_c' and loss modulus G_c'' are obtained in rheological measurements and determine the elastic and dissipative properties of the confined system.

It has been demonstrated [15–17] that the observed response of the internal, embedded, system strongly depends on the choice of external, mechanical, parameters of surface forces apparatus. It is therefore important to analyze the rheological and tribological responses of the system in different ranges of the external parameter space. Since in rheological measurements the drive is oscillatory, one can fix the amplitude/frequency and vary the frequency/amplitude. These correspond to the different lines drawn across the phase diagram in Fig. 1b. In order to probe the rheological properties of an embedded system, the interaction of the top plate with the molecular chain should be dominant, so that $\alpha < 1$. For small driving amplitudes, A_d, the displacement amplitude of the plate, $|\overline{Y}|$, is smaller than the period of the surface potential, and the response of the system is linear. The eigenfrequency of the top plate, $\sqrt{\alpha_p^2(\rho, \Delta) + \alpha^2}$, depends on the external springs, elastic properties of the chain, and misfit parameter Δ. For noninteracting particles the parameter $\alpha_p^2 = 1/2$ [18]. This frequency corresponds to the broken line, $V_d = \sqrt{\alpha_p^2 + \alpha^2}\, A_d$, in Fig. 1b. There is no analog to such a linear response in tribological experiments performed under constant driving velocity. After exceeding a critical driving amplitude, A_{dc}, the top plate executes oscillations with an amplitude $|\overline{Y}|$ larger than the potential period. In Fig. 1b the dotted vertical line $A_d = A_{dc}$ divides the phase diagram into undercritical and overcritical amplitude regimes. The critical amplitude A_{dc} can be estimated to be $A_{dc} \approx F_s/(K_1 b)$, where F_s is the static friction force obtained from tribological experiments.

For values of the driving amplitude in the range $V_c/\delta \gtrsim A_d \gtrsim A_{dc}$ the system exhibits a nonlinear behavior. V_c is the critical driving velocity which denotes the transition to sliding in constant velocity measurements. The different "phases" in Fig. 1b can be related therefore to the tribological observations F_s and V_c [1,4,5,7–9]. For very high driving amplitudes, $A_d > V_c/\delta$, the system again follows linear response but with an eigenfrequency, α, different than that in the low amplitude region. This frequency corresponds to the dash-dotted line $V_d = \alpha A_d$ in Fig. 1b. Here the top plate feels only the spring system and not the interaction with the embedded system. Experimentally, in order to be dominated by the properties of the embedded systems, one should choose frequencies below the eigenfrequencies in each regime, as shown schematically by the shaded area in Fig. 1b.

Figure 2 illustrates a case where the response of the system is nonlinear. In the corresponding regime, $V_c/\delta \gtrsim A_d \gtrsim A_{dc}$, the top plate displacements Y and the spring force f_s demonstrate stick-slip behavior. This is also mirrored by the top plate velocity which clearly shows fast events with $\dot{Y} \gg V_d$. We observe that in the slip windows the chain length displays contractions separated by stick windows with the undisturbed chain configuration.

The main output of rheological experiments is the complex modulus G_c [see Eq. (5)] from which an effective viscosity can be obtained [10–12,14]. Figure 3 shows the storage modulus G_c' and the loss modulus G_c'' as a function

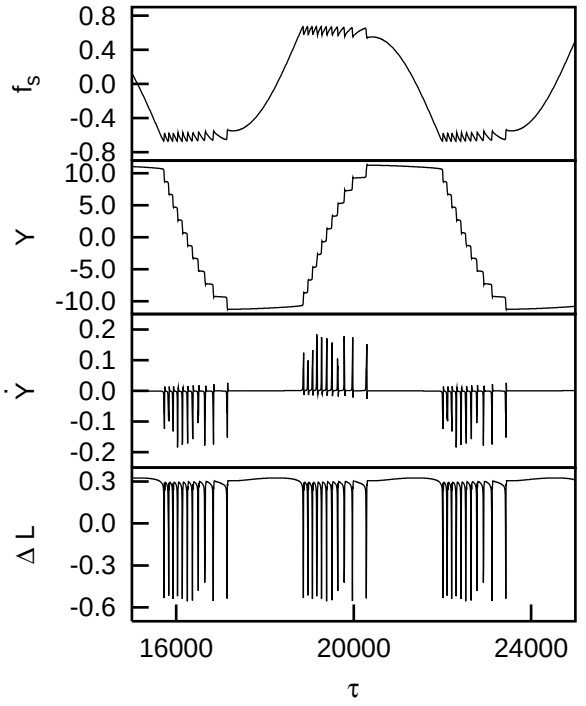

FIG. 2. Time dependence of the spring force f_s, the top plate displacement Y and velocity $\dot{Y}$, and the embedded chain deformation, ΔL, for the driving amplitude $A_d = 40$ and frequency $\delta = 0.001$ (all values are dimensionless). Other relevant parameters are $\varepsilon = 0.01$, $\alpha = 0.1$, $\gamma = 1.0$, $\kappa = 0.5$, $\rho = 1$, $\Delta = 0.1$, and $N = 15$.

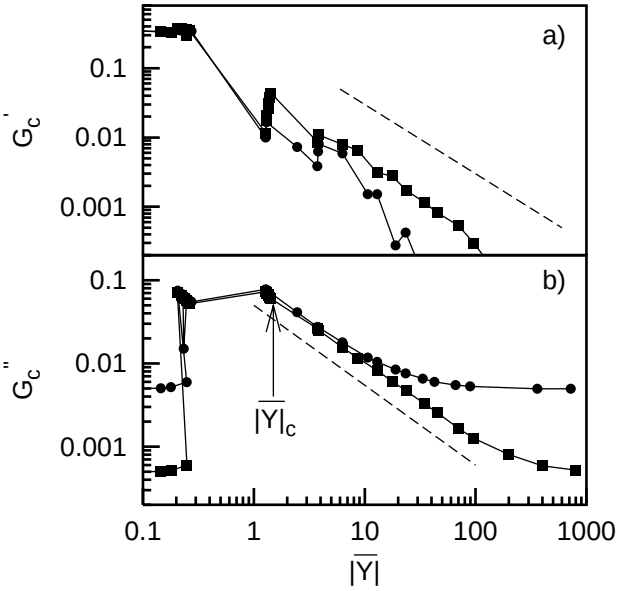

FIG. 3. The dependence of the storage G_c' (a) and loss G_c'' (b) moduli on the amplitude of the top plate displacement $|\overline{Y}|$. The dependence is obtained for two driving frequencies: $\delta_1 = 0.001$ (squares) and $\delta_2 = 0.01$ (circles). All other parameters are the same as in Fig. 2. The dashed lines show the slope -1.

of the amplitude of the top plate displacement (strain) for two different driving frequencies. We now show that from the analysis of the moduli one can deduce some unknown internal parameters of the system. In Fig. 3 one can clearly distinguish among three regimes which correspond in the phase diagram, Fig. 1b, to $A_d < A_{dc}$, $A_{dc} < A_d < V_c/\delta$, and $A_d > V_c/\delta$. Namely, we find two linear regimes, $|\overline{Y}| \ll 1$ and $|\overline{Y}| \gg 1$, where the system responds linearly, and an intermediate nonlinear regime, $|\overline{Y}| \gtrsim 1$. According to our model the measurements of G_c' and G_c'' for $|\overline{Y}| \ll 1$ give $G_c' = \alpha_p^2$ and $G_c'' = \gamma\delta/2$, which in dimensional representation corresponds to $G_c' = 4\pi^2\alpha_p^2 N U_0/b^2$ and $G_c'' = N\eta_0\omega_d/2$. From these measurements one readily obtains the microscopic parameters $N\eta_0$ and NU_0/b^2. From the value of the critical amplitude A_{dc} and from G_c', one can estimate the periodicity of the chain-plate interaction $U(x)$. In the $|\overline{Y}| \gg 1$ regime $G_c' \approx 0$ and $G_c'' = \gamma\delta/2$.

An interesting feature of the loss modules in Fig. 3 is the abrupt increase of G_c'' at the critical displacement A_{dc} followed by a decrease with $|\overline{Y}|$, which is a manifestation of the shear thinning effect. The increase of G_c'' is related to a corresponding increase in dissipation. The latter originates from the stick-slip motion in this range of $|\overline{Y}|$, which leads to a strong energy dissipation during fast slip events seen in Fig. 2. Assuming that the length, l, and the energy loss, E_0, during each slip event are practically independent of the external drive, we can roughly estimate the energy loss, W, during a period of the driving oscillations, $T = 2\pi/\delta$. For the driving velocities, $A_d\delta$, which are below the critical velocity V_c, the number of stick-slip events is proportional to A_d/l, so that the energy loss is $W \propto E_0 A_d/l$. As a result we have

$$G_c'' \propto W/|\overline{Y}|^2 \propto E_0/l|\overline{Y}|\,. \tag{6}$$

This scaling behavior of G_c'' with $|\overline{Y}|$, and the independence of δ, is observed in Fig. 3b for $|\overline{Y}|_c < |\overline{Y}| < V_c/\delta$. Note that stick slip occurs only for velocities below V_c. As the amplitude of the displacement keeps growing we arrive in the regime where two phases, stick-slip and smooth sliding, coexist under the condition of oscillatory drive. These two phases compete as channels for dissipation, and the relative weight of the stick slip compared to smooth sliding is reduced when $|\overline{Y}|$ increases. For $V_d > V_c$, during a displacement of length A_d, stick-slip motion occurs in the interval $A_d V_c/V_d$ and the number of stick slips equals $V_c/l\delta$. Namely, the contribution of the stick-slip phase to the energy loss during this period is $W_{SS} \propto E_0 V_c/l\delta$. The contribution from the smooth sliding is $W_{SL} \propto (\gamma\delta|\overline{Y}|^2/2)[1 - f(V_c/\delta|\overline{Y}|)]$, where $f(z) \equiv 2(\arcsin z - z\sqrt{1 - z^2})/\pi$. In this transition regime we get

$$G_c'' \propto \frac{\gamma\delta}{2} + \frac{\delta E_0}{V_c l}\left[\left(\frac{V_c}{\delta|\overline{Y}|}\right)^2 - \frac{\gamma V_c l}{2E_0} f\left(\frac{V_c}{\delta|\overline{Y}|}\right)\right], \tag{7}$$

which leads to the behavior shown in Fig. 3b for $|\overline{Y}| > V_c/\delta$. The larger is the displacement $|\overline{Y}|$, the smaller

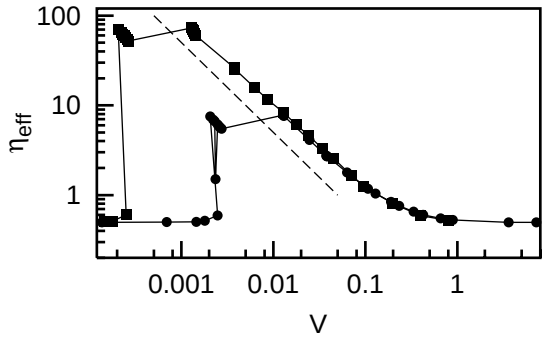

FIG. 4. The dimensionless effective viscosity $\eta_{\text{eff}} = G_c''/\delta$ as a function of the top plate velocity (strain), $V = |\overline{Y}|\delta$. Notations and parameters are as in Fig. 3.

is the relative contribution of the stick slip. For $|\overline{Y}| \gg V_c/\delta$ we arrive at $G_c'' \approx \gamma\delta/2$, which is characteristic for smooth sliding typical of "liquid"-like systems.

In addition to the scaling of G_c'' with $|\overline{Y}|$, it follows from Eqs. (6) and (7) that the effective viscosity $\eta_{\text{eff}} = G_c''/\delta$ scales with the velocity of the top plate, $V \equiv |\overline{Y}|\delta$, in the thinning regime. Figure 4 supports this result and clearly shows that curves which belong to different δ values collapse in the thinning regime as a function of velocity. Using $|\overline{Y}|\delta$ as a meaningful velocity in the case of oscillatory drive is, therefore, justified only in this thinning regime. For lower values of this velocity the behavior depends on the actual values of δ and/or $|\overline{Y}|$. An immediate conclusion from Fig. 4 is that the maximal value of η_{eff} depends on δ. Namely, the choice of the driving frequency, δ, determines this observed maximal value, which is not an inherent property of the embedded system. This can explain the controversial observations of the enhanced viscosity at low velocities [3,6]. Also the velocity at which thinning sets in appears to depend on δ.

Similar behaviors of G_c', G_c'', and η_{eff}, as shown in Figs. 3 and 4, including the scaling properties, have been observed experimentally [10–12]. The experiments report an inverse power law dependence of η_{eff} on velocity, $\eta_{\text{eff}} \propto 1/V$, which follows directly from Eq. (6) as $\eta_{\text{eff}} \propto E_0/\delta|\overline{Y}|$.

The predicted properties of the harmonically driven system should be amenable to experimental tests. In particular, we propose investigations of the shear moduli at low driving amplitudes from which one can deduce microscopic scale parameters, such as the friction constant η, the effective amplitude U_0, and period b of the substrate potential. These parameters characterize the system for all driving amplitudes. Our interpretation of the mechanism that leads to shear thinning, which occurs at higher amplitudes, can be verified by careful analysis of the spring force time series. This can be done, for instance, by studying the corresponding power spectrum [19].

The authors are grateful for helpful discussions with Mike Drake, Steve Granick, and Jacob Klein. Financial support for this work by the Israel Science Foundation and the GIF and DIP grants is gratefully acknowledged.

*Permanent address: Department of Physics, State University of Moldova, Mateevici Str. 60, MD-2009, Chişinau, Republic of Moldova.

[1] B. N. J. Persson, *Sliding Friction. Physical Properties and Applications* (Springer-Verlag, Berlin, 1998).
[2] H. Yoshizawa, P. McGuiggan, and J. Israelachvili, Science **259**, 1305 (1993).
[3] H.-W. Hu, G. A. Carson, and S. Granick, Phys. Rev. Lett. **66**, 2758 (1991).
[4] B. Bhushan, J. N. Israelashvili, and U. Landman, Nature (London) **374**, 607 (1995).
[5] P. A. Thomson, M. O. Robbins, and G. S. Grest, Isr. J. Chem. **35**, 93 (1995).
[6] J. Klein and E. Kumacheva, Science **269**, 816 (1995).
[7] Y. Braiman, F. Family, and G. Hentschel, Phys. Rev. B **55**, 5491 (1997).
[8] J. M. Carlson and A. A. Batista, Phys. Rev. E **52**, 4153 (1996).
[9] M. G. Rozman, M. Urbakh, and J. Klafter, Phys. Rev. Lett. **77**, 683 (1996).
[10] Y.-K. Cho and S. Granick, Wear **200**, 346 (1996).
[11] G. Luengo, J. Israelachvili, and S. Granick, Wear **200**, 328 (1996).
[12] G. Luengo, F.-J. Schmitt, R. Hill, and J. Israelachvili, Macromolecules **30**, 2482 (1997).
[13] J. Peachey, J. V. Alsten, and S. Granick, Rev. Sci. Instrum. **62**, 462 (1991).
[14] J. D. Ferry, *Viscoelastic Properties of Polymers* (John Wiley & Sons, Inc., New York, 1970).
[15] A. D. Berman, W. A. Ducker, and J. N. Israelachvili, Langmuir **12**, 4559 (1996).
[16] M. G. Rozman, M. Urbakh, and J. Klafter, Phys. Rev. E **54**, 6485 (1996).
[17] M. G. Rozman, M. Urbakh, and J. Klafter, Europhys. Lett. **39**, 183 (1997).
[18] $\sqrt{\alpha_p^2 + \alpha^2}$, the dimensionless frequency of the small oscillations of the top plate can be obtained from the solution of the linearized equations of motion, Eq. (1).
[19] A. L. Demirel and S. Granick, Phys. Rev. Lett. **77**, 4330 (1996).